Vietnam Journal of Mechanics, Vol. 46, No. 3 (2024), pp. 229 – 239
DOI: https://doi.org/10.15625/0866-7136/21024

DESIGN OF A VARIABLE STIFFNESS ACTUATOR BASED ON A MULTI-PULLEY SYSTEM WITH A SPRING

Dong Anh Khoa To[1], **Hoang Phuc Chau**[1], **Vu Linh Nguyen**[1,2,*]
[1]*College of Engineering and Computer Science, VinUniversity, Hanoi, Vietnam*
[2]*VinUni-Illinois Smart Health Center, VinUniversity, Hanoi, Vietnam*
[*]E-mail: linh.nv2@vinuni.edu.vn

Received: 29 February 2024 / Revised: 14 May 2024 / Accepted: 28 June 2024
Published online: 30 September 2024

Abstract. This paper presents a variable stiffness actuator (VSA) based on a multi-pulley system with a linear spring. In this design, twelve pairs of outer pulleys and six pairs of inner pulleys are evenly arranged around a center and are serially connected to a spring through a cable. When the inner pulleys rotate about the center point, the spring is extended to generate an elastic force exerted on the cable and then transmitted to the output link as an output torque, resulting in an output stiffness. The significance of the proposed design is that it can quickly vary the output stiffness by adjusting the positions of the inner pulleys using a cam disk. Also, all the components are adequately arranged, making the design compact. In this work, the design concept, analysis, and a numerical example are provided to illustrate the proposed VSA and its performance. It is shown that the VSA can offer a maximum output torque of 30 N-cm with a maximum deflection of 40 degrees. These parameters can demonstrate the wide application and high adaptability of the proposed actuator to various environments.

Keywords: variable stiffness, spring design, pulleys, nonlinear torque, actuator design.

1. INTRODUCTION

The variable stiffness design is inspired by the challenges of replicating human joints for robotic applications and the debilitation of human joints after unfortunate accidents. Variable stiffness actuators (VSAs) have a wide range of applications, from robotic joints to human support devices like exoskeletons. Many designs have been introduced using various types of springs and arrangements, such as the coiled extension spring [1], flexible components [2], coiled compression spring [3–5], and leaf springs [6–8].

The design in [1] uses a series of pulleys that can be changed based on the requirements of the applications. Half of the springs connect to the output section, and the rest are fixed to the input flange. The whole mechanism is connected using a wire that has one end fixed to a winding mechanism and the other fixed to a spring. This mechanism has a significant flaw in that the wire could easily slip out of the pulleys during operations due to the unstable connections between the pulleys and the wire. The work in [2] proposed a detailed analysis of customized coiled compression springs with an S-shape. This is a more efficient configuration that allows more angles of freedom compared to others, but it is too complex and requires an extensive number of components to produce. Leaf springs have also been used in VSAs [6–8]. They have similar working principles with a roller bearing, which is responsible for changing the effective length of the leaf spring and thus varying the stiffness of the whole structure.

In this paper, we propose a new design concept for a VSA based on a multi-pulley system with a linear spring. In this design, the change in the output stiffness is achieved by adjusting the position of the inner pulleys using a cam disk. The significance of this principle is that it can vary the output stiffness quickly and provide a wide range of output stiffness that makes it suitable for many applications, especially for knee-joint exoskeleton. In this work, we will provide a theoretical model of the VSA and demonstrate its performance via a numerical example.

2. DESIGN CONCEPT

Fig. 1 illustrates the overall design of the proposed VSA and its application to a knee-joint exoskeleton. In this model, the upper part (denoted by the pink color) is attached to the thigh, while the yellow one is placed on the leg. The proposed actuator can be used to support people with weakened knee joints, for example, to help them regain the functionality of the knee joints.

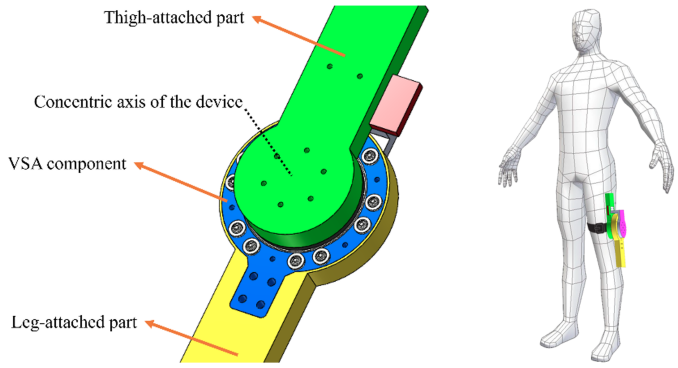

Fig. 1. The overall design of the proposed VSA and its application to a knee-joint exoskeleton

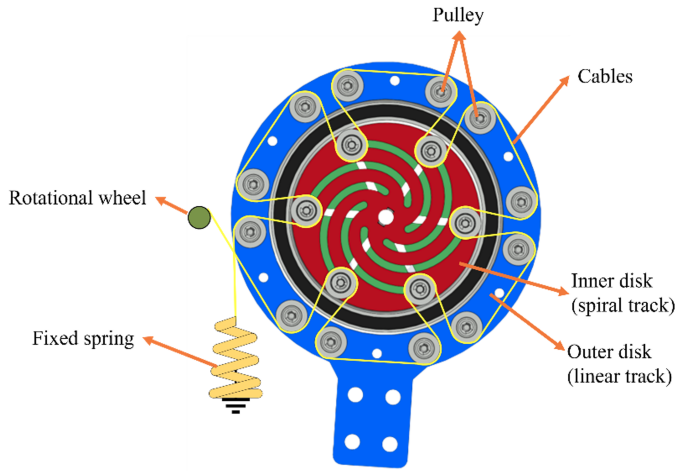

Fig. 2. Structure of the proposed VSA

The design of the VSA was inspired by the iris shutter mechanism. For the purpose of changing the stiffness when varying the angle of deflection between two linkages, a pulley-cable system has been introduced (Fig. 2). Specifically, it consists of two disks. The bigger part consists of 12 pulleys and 6 linear tracks distributed equally in a hexagon. Meanwhile, there are also 6 pulleys for the inner one, but the tracks are spiral-shaped. A string-like cable stemming from a fixed spring will go through the pulleys and end at a rotational wheel. When the outer disk is deflected, specifically during the swing phase of the knee, the spring is forced to extend; as a result, an elastic force will be generated to oppose the change and align again the two disks, which in turn provides supportive torque for the patient. What makes this design advanced is the ability to vary spring stiffness, particularly through adjustment of the resultant's disk pulley position. For consistency, the outer disk is denoted as the "initiating disk" and the inner is called the "resultant disk".

The main principle is that whenever the stiffness needs to be adjusted, the position of the inner pulley would be changed accordingly due to the rotation of a smaller disk driving by a particular motor. Because the pulleys are placed simultaneously in 2 tracks, the spiral rays would drive the pulley along the linear ones, as shown in Fig. 3. Additionally, stiffness control could be achieved by varying the preload of the tension spring. In this model, a total of 6 groups (2 outer pulleys and 1 inner pulley) are introduced. However, this design can be modified to match the purposes of its use. For instance, a work that requires higher stiffness may need more pulley, while lighter jobs can have less to reduce the weight of the overall devices. The advantage of this product is that it can be easily dismantled and installed, providing high reconfigurability and allowing it to perform in a wide range of torque.

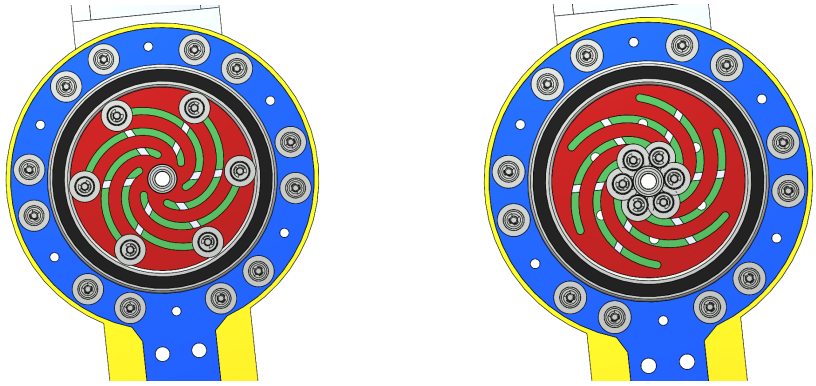

(a) Initial position of inner pulley (b) Subsequent positions of inner pulleys

Fig. 3. Stiffness variation with different track shapes

3. THEORETICAL ANALYSIS

This section presents two analytical approaches for the proposed VSA. The first uses geometrical calculations, while the other uses the vector-based principle. To reduce the complexity of the calculation, two assumptions are made: (i) the pulley centers are connected by a straight cable, and (ii) the torque generated by each pulley group (two outer pulleys and one inner pulley) is consistent among all the locations. Therefore, the analysis must be conducted in one group and then generalized for N groups. Fig. 4 shows the chosen pulley group for the current analysis. The objective of this section is to analyze the relationship between the output torque and deflected angle, resulting in the output stiffness, and how to change the output stiffness in this design.

Fig. 4. The chosen pulley group for the current analysis

3.1. Geometrical analysis

Fig. 5 illustrates the geometrical diagram for the selected pulley group. When the outer disk deflects an angle of θ, the transitional pulley moves from point C to point D. This movement changes the length of the connecting cable between the fixed and transitional pulleys, which are denoted as l_1, l_2. Thus, two elastic forces along the cable are calculated as

$$F_1 = k\,(l_1 - l_0) + P_0, \tag{1}$$

$$F_2 = k\,(l_0 - l_2) + P_0, \tag{2}$$

where k is the stiffness of the spring, and P_0 is the pre-extension of the spring.

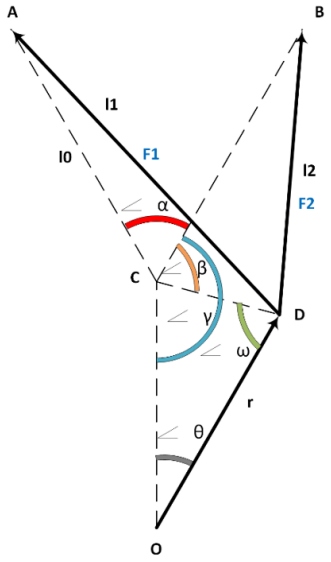

- O = Center point of two disks.
- C = Temporary position of the transitional pulley.
- A, B = Fixed pulleys on the outer disk.
- r = Radius of the inner disk, constant.
- l_0 = The length of initial state of the cable, $l_{AC} = l_{BC}$, constant.
- l_1, l_2 = The length of subsequent state of the cable after the inner disk deflects a certain angle, $l_1 = l_{AD}, l_2 = l_{BD}$.
- F_1, F_2 = Force due to the extension of the spring, acting along the cable line.
- α: Angle between two cables in the initial position, constant.
- θ: Deflected angle of the outer disk.
- β, ω, γ: angle variable.

Fig. 5. Geometrical diagram for one group pulley

From Fig. 5, the angle γ can be determined as

$$\gamma = \frac{360 - \alpha}{2} = 180^\circ - \frac{\alpha}{2}. \tag{3}$$

Consider the isosceles triangle ΔOCD, the angle ω is calculated as

$$\omega = \frac{180^\circ - \theta}{2} = 90^\circ - \frac{\theta}{2}. \tag{4}$$

Therefore, based on the diagram, β is calculated by

$$\beta = \gamma - \omega = 180^\circ - \frac{\alpha}{2} - \left(90^\circ - \frac{\theta}{2}\right) = 90^\circ + \frac{\theta}{2} - \frac{\alpha}{2}. \tag{5}$$

Combine α and β, we get the angle $\angle ACD$

$$\angle ACD = \alpha + \beta = 90^\circ + \frac{\theta}{2} - \frac{\alpha}{2} + \alpha = 90^\circ + \frac{\theta + \alpha}{2}. \tag{6}$$

Apply the cosine principle in ΔACD, and with the estimation of $CD = r \times \theta$, l_1 is calculated by

$$l_1 = \sqrt{(r\theta)^2 + l_0^2 - 2r\theta l_0 \cos(\angle ACD)}. \tag{7}$$

Replace the value of $\angle ACD$ into the equation with $\cos(90 + x) = -\sin(x)$, the result is

$$l_1 = \sqrt{(r\theta)^2 + l_0^2 + 2r\theta l_0 \sin\left(\frac{\theta + \alpha}{2}\right)}. \tag{8}$$

Since the direction of F_1 goes in the direction of DA, the torque caused by this force is

$$\tau_1 = \vec{F_1} \times \vec{r} = |F_1||r| \sin(180^\circ - \angle ADO) = |F_1||r| \sin(\angle ADO). \tag{9}$$

To calculate $\angle ADO$, firstly, $\angle ADC$ needs to be determined by

$$\angle ADC = \arcsin\left(\frac{(\sin(\angle \mathrm{ACD}) \times l_0)}{l_1}\right). \tag{10}$$

Then, $\angle ADO$ is the combination of $\angle ADC$ and ω as

$$\angle ADO = \angle ADC + \omega = \arcsin\left(\frac{(\sin(\angle ACD) \times l_0)}{l_1}\right) + 90^\circ - \frac{\theta}{2}. \tag{11}$$

Finally, the torque generated by F_1 is

$$\tau_1 = \vec{F_1} \times \vec{r} = |F_1||r| \sin(\angle ADO) = k(l_1 - l_0 + P_0)\, r(\sin(\angle ADO)) = f(\theta), \tag{12}$$

where the length l_1 is demonstrated in Eq. (8) and $\angle ADO$ is in Eq. (11). To find the length l_2, the approach is to use the cosine rule in ΔCDB

$$l_2 = \sqrt{(r\theta)^2 + l_0^2 - 2r\theta l_0 \cos(\beta)} = \sqrt{(r\theta)^2 + l_0^2 + 2r\theta l_0 \cos\left(\frac{\theta - \alpha}{2}\right)}. \tag{13}$$

The torque made by F_2 is

$$\tau_2 = \vec{F_2} \times \vec{r} = |F_1||r| \sin(\angle BDO). \tag{14}$$

To find the angle $\angle BDO$, firstly, it is required to find the angle $\angle BDC$ as

$$\angle BDC = \arcsin\left(\frac{(\sin(\beta) \times l_0)}{l_2}\right). \tag{15}$$

Then, the angle $\angle BDO$ is the combination of $\angle BDC$ and ω

$$\angle BDO = \angle BDC + \omega = \arcsin\left(\frac{(\sin(\beta) \times l_0)}{l_2}\right) + 90^\circ - \frac{\theta}{2}. \tag{16}$$

Subsequently, the torque created by F_2 is

$$\tau_2 = \vec{F}_2 \times \vec{r} = |F_2||r| \sin(\angle BDO) = k(l_0 - l_2 + P_0)\, r(\sin(\angle BDO)) = g(\theta). \tag{17}$$

The net torque of this pulley group is the subtraction of two independent torques generated by two cables as they are in opposite directions. To calculate the full VSA, the formula must be multiplied by N (i.e., the number of groups). Hence, the net moment of the VSA is calculated as

$$\tau_{net} = N(\tau_1 - \tau_2) = N(f(\theta) - g(\theta)), \tag{18}$$

or equivalently,

$$\tau_{net} = N(k(l_1 - l_0 + P_0)\, r(\sin(\angle ADO)) - k(l_0 - l_2 + P_0)\, r(\sin(\angle BDO))). \tag{19}$$

3.2. Vector-based analysis

For convenient calculations, we will attach the coordinate system to the design as shown in Fig. 6. The two outer pulleys will be assigned as (2; 10) and (−2; 10) with the centimeter unit. The initial position of the inner pulley is $(0; r_0)$, with r_0 being the distance from the center, which is also the radius of rotation of the inner disk. This section also considers one group first before generalization.

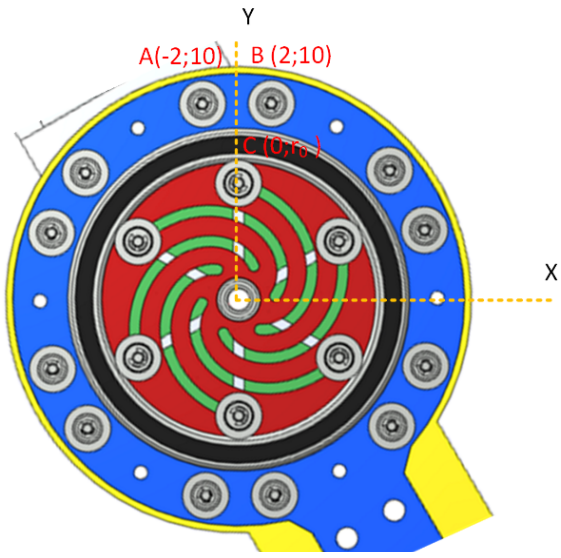

Fig. 6. Coordinate system for vector-based analysis

Firstly, the initial length of cable, l_0, is determined as

$$l_0 = \sqrt{(2-0)^2 + (10-r_0)^2}, \tag{20}$$

with a deflected angle of θ, the position of the inner pulley (point D) is tracked by the vector

$$\vec{r} = [r_0 \sin(\theta); r_0 \cos(\theta)]. \tag{21}$$

The coordination vector of cable DA is determined as

$$\vec{DA} = [-2 - r_0 \sin(\theta); 10 - r_0 \cos(\theta)]. \tag{22}$$

As the length of the vector $\vec{DA}$ is $|\vec{DA}|$, the unit vector of DA is defined as

$$u_{\vec{DA}} = \frac{\vec{DA}}{|\vec{DA}|}. \tag{23}$$

The force acting along DA is calculated as

$$F_{\vec{DA}} = k\left(\left|\vec{DA}\right| - l_0 + P_0\right) \times u_{\vec{DA}}. \tag{24}$$

From this, associating torque can be found by

$$\tau_{\vec{DA}} = \vec{\tau_1} = \vec{r} \times F_{\vec{DA}} = k\left(\left|\vec{DA}\right| - l_0 + P_0\right)(\vec{r} \times u_{\vec{DA}}). \tag{25}$$

Similarly, the coordination vector of DB is expressed as

$$\vec{DB} = [2 - r_0 \sin(\theta); 10 - r_0 \cos(\theta)]. \tag{26}$$

The corresponding torque is calculated as

$$\tau_{\vec{DB}} = \vec{\tau_2} = \vec{r} \times F_{\vec{DB}} = k\left(l_0 - \left|\vec{DA}\right| + P_0\right)(\vec{r} \times u_{\vec{DB}}). \tag{27}$$

From this, the magnitude of the general torque of the system can be determined by

$$\tau_{net} = N(|\vec{\tau_1}| - |\vec{\tau_2}|). \tag{28}$$

This method has reduced the complexity of calculations, making it easier to simulate the performance and validate the results.

3.3. Output stiffness

The total torque of the system has the form: $\tau_{net} = f(\theta)$; however, this is the combination of both cable extension and pre-extension of spring. For deeper analysis, it is required to separate such two contributors. This can be achieved by simply canceling out one element in the force formula; e.g., in cable DA, the extension of due to cable is $\left|\vec{DA}\right| - l_0$, while that of pre-extension is just basically P_0.

The formula can be rewritten as

$$\tau_{net} = f_1(\theta) + f_2(\theta), \tag{29}$$

with $f_1(\theta)$ and $f_2(\theta)$ are the involvement of cable and pre-extension, respectively. Now, the stiffness of each component can be determined by simply dividing by the deflected angle θ as

$$k_{net} = \frac{f_1(\theta)}{\theta} + \frac{f_2(\theta)}{\theta} = k_1 + k_2. \tag{30}$$

4. NUMERICAL ANALYSIS

The parameters of the VSA in the numerical analysis are given as follows: The angle θ ranges from 0 to 40 degrees; four values of r_0, corresponding to four different positions from the center, are assessed as r_0 = 1, 3, 5, 7 cm; the stiffness coefficient of the spring is k = 0.12 N/cm, the pre-extension is P_0 = 5 cm, and the number of pulley groups is N = 6. Fig. 7 shows the output torques with different positions of inner pulleys. The first impression is that the further it is from the center, the higher the torque achieved. This aligns with our intuitive prediction as the longer the distance is, the greater stiffness exists. It can be observed that from θ = 0 to θ = 10 degrees, the torques generated by both four values of r_0 increase linearly. However, from θ = 10 to θ = 20 degrees, the four lines remain relatively horizontal, which means that the change in torque is not significant, and there is even a small decline in the line corresponding to a 7 cm distance from the center. However, after θ = 25 degrees, that line is recorded as the most dramatic growth, while the rate of change reduces linearly with respect to the distance. In other words, the further the distance is, the more significant the torque produced after θ = 25 degrees.

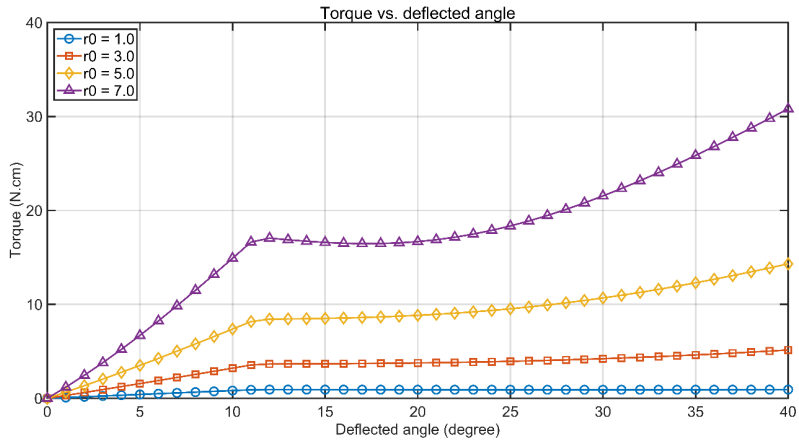

Fig. 7. Output torques with different positions of inner pulleys

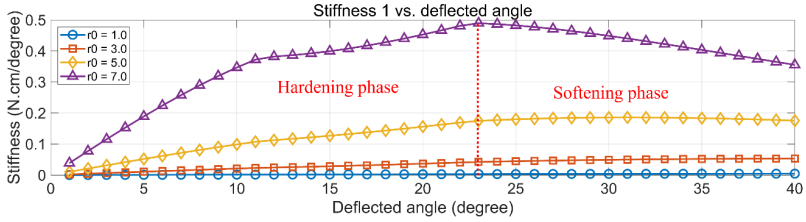

(a) Type-1 stiffness due to the cable extension

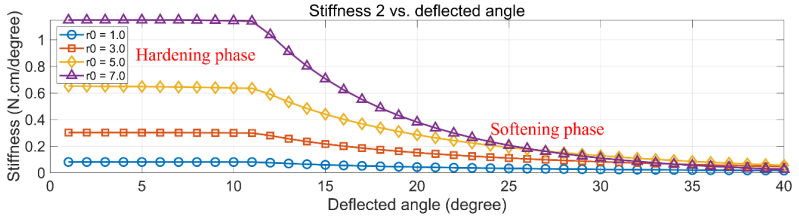

(b) Type-2 stiffness due to the spring pre-extension

Fig. 8. Stiffness behavior of the VSA

Fig. 8 illustrates the stiffness behavior of the VSA. As can be seen, the region can be divided into sub-components: hardening and softening phases. In Fig. 8(a), the stiffness increases when the deflected angle increases, representing the hardening period. After that, a declining trend is obtained and denoted as the softening phase. Fig. 8(b) represents a decreased trend of stiffness. Beginning with a relatively constant value, the stiffness plunges and nearly reaches 0 at 40 degrees. From these results, it can be observed that there is a peak of type 1 stiffness due to geometry at around 23 degrees. Possibly, this is the location where the distance from point B to the inner pulley (point D) is smallest (as point B is fixed, but the inner pulley runs in a circle). Furthermore, the preload due to pre-extension does affect the overall stiffness considerably. Hence, to tune the hardening and softening phases of the mechanism, the number of pulley groups or the setup of the initial condition of the spring can be adjusted, leading to high flexibility and reconfigurability of the device.

5. CONCLUSION

This paper introduced a new design concept for a VSA using a multi-pulley system with a linear spring. The proposed VSA provides a varying stiffness, which was achieved by using a cam disk to change the positions of the inner pulleys, and its change was quickly obtained. In this work, the design concept, analysis, and a numerical example were presented to demonstrate the proposed VSA and its performance. It was presented that the VSA offered a maximum output torque of 30 N-cm with a maximum

deflection of 40 degrees. However, the optimal working range will be up to 23 degrees. The obtained outputs demonstrated the wide application and high adaptability of the proposed design to various environmental conditions. Future research may include integrating this mechanism into developing rehabilitative devices, targeting stroke patients to support them during recovery.

DECLARATION OF COMPETING INTEREST

The authors declare that they have no known competing financial interests or personal relationships that could have appeared to influence the work reported in this paper.

ACKNOWLEDGEMENT

The authors appreciate the support from VinUni-Illinois Smart Health Center, VinUniversity, Hanoi, Vietnam.

REFERENCES

[1] Y. Zhu, Q. Wu, B. Chen, D. Xu, and Z. Shao. Design and evaluation of a novel torque-controllable variable stiffness actuator with reconfigurability. *IEEE/ASME Transactions on Mechatronics*, **27**, (2022), pp. 292–303. https://doi.org/10.1109/tmech.2021.3063374.

[2] L. Fang and Y. Wang. Stiffness analysis of a variable stiffness joint using a leaf spring. In *Lecture Notes in Computer Science*, Springer International Publishing, (2017), pp. 225–237. https://doi.org/10.1007/978-3-319-65292-4_20.

[3] Y. Liu, S. Cui, and Y. Sun. Mechanical design and analysis of a novel variable stiffness actuator with symmetrical pivot adjustment. *Frontiers of Mechanical Engineering*, **16**, (2021), pp. 711–725. https://doi.org/10.1007/s11465-021-0647-1.

[4] T. Bacek, M. Moltedo, C. Rodriguez-Guerrero, J. Geeroms, B. Vanderborght, and D. Lefeber. Design and evaluation of a torque-controllable knee joint actuator with adjustable series compliance and parallel elasticity. *Mechanism and Machine Theory*, **130**, (2018), pp. 71–85. https://doi.org/10.1016/j.mechmachtheory.2018.08.014.

[5] C. Wang, B. Sheng, Z. Li, M. Sivan, Z.-Q. Zhang, G.-Q. Li, and S. Q. Xie. A lightweight series elastic actuator with variable stiffness: Design, modeling, and evaluation. *IEEE/ASME Transactions on Mechatronics*, **28**, (2023), pp. 3110–3119. https://doi.org/10.1109/tmech.2023.3254813.

[6] Y. Xu, K. Guo, J. Sun, and J. Li. Design, modeling and control of a reconfigurable variable stiffness actuator. *Mechanical Systems and Signal Processing*, **160**, (2021). https://doi.org/10.1016/j.ymssp.2021.107883.

[7] Y. Lu, Y. Yang, Y. Xue, J. Jiang, Q. Zhang, and H. Yue. A variable stiffness actuator based on leaf springs: Design, model and analysis. *Actuators*, **11**, (2022). https://doi.org/10.3390/act11100282.

[8] D. J. Braun, V. Chalvet, T.-H. Chong, S. S. Apte, and N. Hogan. Variable stiffness spring actuators for low-energy-cost human augmentation. *IEEE Transactions on Robotics*, **35**, (2019), pp. 1435–1449. https://doi.org/10.1109/tro.2019.2929686.